J Mater Sci

Chemical routes to materials

Viologen capped by nucleobase—building blocks for functional materials: synthesis and structure–properties relationship

Marius Ciobanu[1] and Carmen-Simona Jordan[2,*]

[1] *Department of Organic Materials Chemistry, Institute of Chemistry of New Materials, University of Osnabrück, 79074 Osnabrück, Germany*

[2] *Chemistry and Chemical Engineering Faculty Management Culture and Technology, University of Applied Sciences, 49076 Osnabrück, Germany*

Received: 31 May 2021
Accepted: 21 September 2021

ABSTRACT

The current study presents a new class of functional derivatives (**1–3**) consisting of a dicationic viologen (4,4′-bipyridinium unit) ($\mathbf{V^{2+}}$) capped by nucleobases thymine ($\mathbf{NB_1}$), adenine ($\mathbf{NB_2}$), thymine/adenine ($\mathbf{NB_1}$, $\mathbf{NB_2}$), and ion-paired with amphiphilic anion 3,4,5-tris(dodecyloxy)benzene sulfonate ($\mathbf{DOBS^-}$). The target of our work focuses on the design and synthesis of molecular building blocks in which three different functionalities are combined: chromophore ($\mathbf{V^{2+}}$ unit), molecular recognition (**NB** unit), and thermotropic liquid crystal (**DOBS** unit). The resulted materials exhibit liquid crystalline properties at ambient temperature with significant particularities-induced by nucleobases in the mesogen structure. Structure–properties relationship study focuses on providing knowledge about (1) how the thermotropic, redox properties, thermochromism, or ionic conductive properties are influenced by the presence of purinic or pyrimidinic nucleobases, and (2) how effective is their ability to self-assembly by hydrogen bonding in nonpolar solvents. The presence of nucleobases has been proved to have a substantial impact on electron transfer rate during the reduction of viologen moieties by intermolecular aggregation. Ionic conductivity and thermochromic properties of derivatives **1–3** were investigated and compared to a non-containing nucleobase analog methyl viologen with 3,4,5-tris(dodecyloxy)benzene sulfonate anion (**MV**) as reference.

Handling Editor: David Cann.

Address correspondence to E-mail: s.jordan@hs-osnabrueck.de

https://doi.org/10.1007/s10853-021-06554-1

Published online: 11 October 2021

Springer

GRAPHICAL ABSTRACT

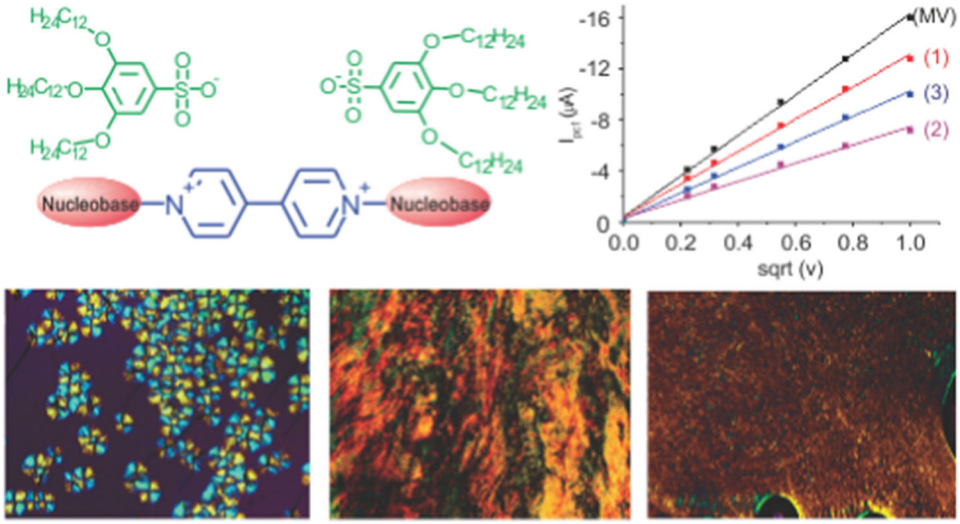

Introduction

Bis-quaternized 4,4′-bipyridinium salts ("viologens") are well-known building blocks of special importance because they allow the generation of functional materials with a multitude of stimuli-induced chromism like electrochromism [1, 2], photochromism [3, 4], thermochromism [5, 6], piezochromism [7], solvatochromism [8]. A particular interest for such compounds lies in their electron [9, 10] or charge transfer [11, 12] abilities. On the other hand, the viologen-based compounds are alternative to the classical ionic organic mesogens such as pyridinium or imidazolium salts [13, 14]. In an ionic liquid crystalline matrix, viologens can be used as multi-stimuli chromic additives to construct "task-specific" materials [15–17]. Recent reports describing viologens capped by alkyl or alkoxy chains exhibit preferentially smectic mesophases[18–20]. Particularly, the mesogenic ionic complexes of polycationic viologens with anionic cunitic ligands such as 3,4,5-tris(dodecyloxy)benzene sulfonate (**DOBS**$^-$) were prepared in our group by phase transfer catalysis [16]. Such materials exhibited LC properties in a broad temperature range (30–270 °C), ionic conductivity in liquid crystalline state, thermo-, and electrochromism. In previous work, we reported the synthesis and study of optoelectronic properties of bifunctional derivatives, so-called *nucleobase-appended viologens*—which combine redox 4,4′-bipyridinium units, with the molecular recognition function of nucleobases thymine (**NB1**) and adenine (**NB2**) [21]. Viologen-nucleobase complexes with 3,4,5-tris(dodecyloxy)benzene sulfonate (**DOBS**$^-$) anions have not

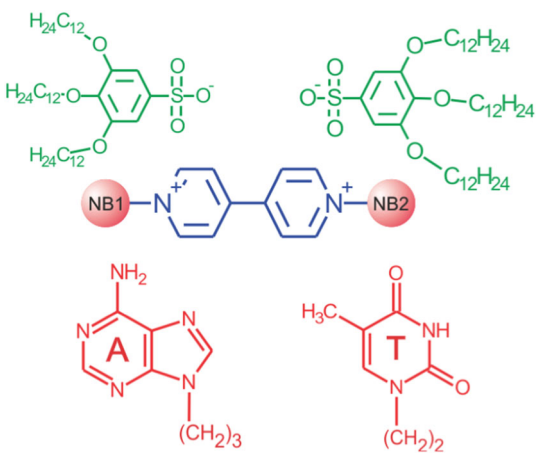

Scheme 1 Chemical structure of nucleobase-appended viologens ion-paired with amphiphilic DOBS$^-$ anion: compound (1) $NB_1 = NB_2 = T$; compound (2) $NB_1 = NB_2 = A$; compound (3) $NB_1 = T$ and $NB_2 = A$.

yet been reported in the literature. The target of our work focuses on the design and synthesis of molecular building blocks with three different functionalities: chromophore ($\mathbf{V^{2+}}$ unit), molecular recognition (**NB** unit), and thermotropic liquid crystal (**DOBS** unit) (Scheme 1).

The bulk solid-state behavior of such complexes, obtained by ion-pairing dicationic nucleobase-appended viologens with amphiphilic anion 3,4,5-tris(-dodecyloxy)benzene sulfonate (**1–3**) was investigated. The systematic structure–properties relationship study focuses on (1) how the thermotropic, redox properties, thermochromism, and ionic conductive properties are influenced by the presence of nucleobases, and (2) how effective is their ability to self-assembly by hydrogen bonding in a nonpolar solvent.

Such multifunctional building-block molecules can form self-assembling structures by ionic interactions, hydrogen bonding, charge transfer, π–π, and van der Waals interactions that have potential applications in nanotechnology, crystal engineering, and medicine.

Experimental section

Synthesis procedure

A solution in water (0.01 mol L^{-1}) of **1**, **2**, or **3**, as iodine salt, was vigorously stirred for 12 h at 21 °C with an equal volume of cesium 3,4,5-tris(dodecyloxy)benzene sulfonate (0.01 mol L^{-1}) solution in chloroform. Further on, the organic phase was separated, washed two times with 20 mL distilled water, dried over $MgSO_4$, and subsequently evaporated under reduced pressure. The resulted yellow solid was freeze-dried from 40 mL benzene to obtain the ionic complexes **1**, **2**, and **3**, respectively.

1,1′-Bis[3-(5-methyl-2,4-dioxo-3,4-dihydropyrimidin-1(2H)-yl)propyl]-4-(pyridin-4-yl)-pyridinium di-[3,4,5-tris(dodecyl)benzene sulfonate] **(1); ^{1}H-NMR** (250 MHz, THF-d_8/D_2O, 4/1 vol.): δ = 9.29 (d, J = 5.34 Hz, 4 H), 8.72 (d, J = 5.34 Hz, 4 H), 7.56 (s, 2 H), 7.05 (s, 4 H), 4.90 (t, J = 6.28 Hz, 4 H), 3.92–4.08 (m, 16 H), 2.54 (quin, J = 7.30 Hz, 4 H), 1.77 (s, 6 H), 1.41–1.57 (m, 12 H), 1.16–1.40 (m, 108 H), 0.86 ppm (t, J = 6.30 Hz, 18 H); **^{13}C-NMR** (62.9 MHz, THF-d_8/D_2O, 4/1 vol.): δ = 165.74(s), 153.50(s), 152.93(s), 151.30(s), 147.04(d), 142.52(d), 141.90(s), 140.25(s), 128.51(d), 111.63(s), 105.73(d), 73.71(t), 69.93(t), 60.30(t), 46.02(t), 32.96(t), 31.51(t), 30.41–31.03(t, overlapped peaks), 27.37(t), 23.64(t), 14.56(q), 12.33 ppm (q); **IR** (ATR, cm^{-1}): 3056(w), 2921(s), 2852(m), 1681(s), 1585(m), 1463(m), 1421(m), 1380(m), 1313(m), 1180(s), 1108(s), 1041(s), 840(m), 721(w), 651(s); **Elemental analysis** calcd (%) for $C_{110}H_{184}N_6O_{16}S_2$ + 2.45 H_2O (1910.8 + 44.1): C 67.95, H 9.41, N 3.92 S 3.34%; found: C 67.58, H 9.74, N 4.3, S 3.28.

1,1′-Bis[2-(6-amino-9H-purin-9-yl)ethyl]-4-(pyridin-4-yl)pyridinium di-[3,4,5-tris(dodecyl) benzene sulfonate]; (**2**); **^{1}H-NMR** (250 MHz, THF-d_8/D_2O, 4/1 vol.): δ = 9.08 (d, J = 6.59 Hz, 4 H), 8.52 (d, J = 6.91 Hz, 4 H), 8.25 (s, 2 H), 7.96 (s, 2 H), 7.05 (s, 4 H), 5.29 (t, J = 5.34 Hz), 5.01 (t, J = 5.34 Hz, 4 H), 3.96 (t, J = 5.97 Hz, 8 H), 3.86 (t, J = 6.28 Hz, 4 H), 1.40—1.56 (m, 12 H), 1.15–1.40 (m, 108 H,), 0.85 ppm (18 H, t, J = 6.28 Hz); ^{13}C-NMR (62.9 MHz, THF-d_8/D_2O, 4/1 vol.): δ = 156.96(s), 153.73(d), 153.52(s), 151.70(s), 150.41(s), 147.50(d), 142.79(d), 141.73(s), 140.26(s), 128.55(d), 119.43(s), 105.72(d), 73.70(t), 69.93(t), 62.13(t), 44.92(t), 32.96(t), 31.52(t), 30.86–30.40(t, overlapped peaks), 27.39(t), 23.64(t), 14.58 ppm (q); **IR** (ATR, cm^{-1}): 3338 (br), 2921(s), 2852(m), 1685(m), 1639(m), 1585(m), 1463(m), 1421(m), 1382(m), 1311(m), 1228(m), 1176(m), 1108(s), 1043(s), 956(w), 836(w), 719(m), 647(s); **Elemental analysis** calcd (%) for $C_{108}H_{178}N_{12}O_{12}S_2$ + 1.85 H_2O (1900.8 + 33.3): C 66.92, H 9.29, N 8.85, S 3.33; found: C 67.07, H 9.47, N 8.69, S 3.32.

1-[2-(6-Amino-9H-purin-9-yl)ethyl]-1′-[3-(5-methyl-2,4-dioxo-3,4-dihydropyrimidin-1(2H)-yl)propyl]-4-(pyridin-4-yl)pyridinium di-[3,4,5-tris (dodecyl)benzene sulfonate] (**3**); ^{1}H-NMR (250 MHz, THF-d_8/D_2O, 4/1 vol.): δ = 9.27 (d, J = 6.59 Hz, 2 H), 9.07 (d, J = 6.59 Hz, 2 H), 8.63 (d, J = 6.59 Hz, 2 H), 8.57 (d, J = 6.91 Hz, 2 H), 8.25 (s, 1 H), 7.96 (s, 1 H), 7.55 (s, 1 H), 7.04 (s, 4 H), 5.29 (t, J = 5.34 Hz, 2 H), 5.01 (t, J = 5.49 Hz, 2 H), 4.88 (t, J = 7.06 Hz, 2 H), 3.77–4.01 (m, 14 H), 2.53 (quin, J = 7.14 Hz, 2 H), 1.78 (s, 3 H), 1.40—1.58 (m, 12 H), 1.12–1.40 (m, 108 H), 0.85 ppm (t, J = 6.28 Hz, 18 H); **^{13}C-NMR** (62.9 MHz, THF-d_8/D_2O, 4/1 vol.): δ = 166.02(s), 157.06(s), 153.87(d), 153.51(s), 153.03(s), 152.01(s), 151.05(s), 150.42(s), 147.40(d), 147.11(d), 142.74(d), 142.65(d), 141.76(s), 140.26(s), 128.59(d), 128.45(d), 119.44(s), 111.79(s), 105.72(d), 73.70(t), 69.93(t), 62.07(t), 60.37(t), 46.03(t), 44.91(t), 32.96(t), 31.52(t), 31.05–30.40(t, overlapped peaks), 27.38(t), 23.64(t), 14.57(q), 12.35 ppm (q); **IR** (ATR, cm^{-1}): 3446 (br), 3058(w), 2921(s), 2852(m), 1681(m), 1639(m), 1585(m), 1463(m), 1421(m), 1380(m),

1313(m), 1228(m), 1180(m), 1108(s), 1043(s), 960(w), 836(w), 651(s); **Elemental analysis** calcd (%) for $C_{109}H_{181}N_9O_{14}S_2 + 1.3\ H_2O$ (1905.8 + 23.4): C 67.72, H 9.42, N 6.40, S 3.38; found: C 67.86, H 9.59, N 6.53, S 3.32.

Molecular characterization

^{1}H- and ^{13}C-NMR spectra were recorded on Bruker AMX-250 spectrometer; ^{1}H: 250 MHz, ^{13}C: 62.9 MHz; chemical shifts δ are given in ppm relative to the solvent signal peaks as internal standard. IR characterization was performed on a Bruker FT-IR Spectrophotometer Vertex 70 by ATR technique. Elemental analyses were made on a VarioMICRO cube device. The content of hygroscopic H_2O was deduced from elemental analysis data by employing JASPER v2.0—JavaScript Percentage Elemental Results Calculator, available online: 15/05/2021 http://www.yorku.ca/pgpotvin/public/Jasper/jasper2.htm.

Thermotropic characterization

DSC measurements were taken on samples of approx. 4–12 mg. Phase transitions were measured on a Netzsch DSC 204 Phoenix differential scanning calorimeter. The heating and cooling rates were 10 °C min^{-1}. Indium, tin, and cyclohexane were used as calibration standards. Thermo-optical polarizing microscopy (TOPM) was realized with a Zeiss AXIOPLAN 2 polarizing microscope, equipped with a Mettler FP 80 hot stage. Pictures were taken using a digital Zeiss AxioCam MRC4 camera with a resolution of 4 megapixels combined with Zeiss AxioVision software.

Diffusion-ordered spectroscopy

DOSY experiments were performed on a Bruker AMX-500 spectrometer using the Bruker pulse program ledbpgp2s. Diffusion time (D20) was 60 ms, the length of the diffusion gradient variable between 600 and 2500 µs (P30) and the gradient recovery delays 200 µs (D16) in deuterated chloroform or THF. Temperature-dependence DOSY measurements were applied to a sample of respective ionic complex **1–3** (50 mM) in the temperature range from 20 to 50 °C. Concentration-dependence DOSY experiments were performed at 30 °C on samples of different concentrations ranging from 3 to 50 mM of ionic complex **1–3**. The deuterated solvent used for temperature and concentration-dependence experiments, respectively, was THF-d_8.

Electrochemical characterization

Cyclic voltammetry experiments were performed under argon in a three-electrode electrochemical cell with the potentiostat PGSTAT 302 N from AUTOLAB controlled by a PC running under GPES from Windows, version 4.9 (ECO Chemie B.V.). A glassy carbon electrode (GCE) from Metrohm (Germany) with an electrochemically active surface area of A = 0.031 cm^2 was used as a working electrode. The surface of the working electrode was polished before the measurement with Al_2O_3. The reference electrode was Ag/AgCl (3 M, KCl in water), and the counter electrode was a Pt wire. The analyte concentration was 1 mmol/L dissolved in THF containing lithium bis(trifluoromethane)sulfonimide (0.1 mol L^{-1}) as a supporting electrolyte.

Ionic conductivity

5–7 mg solid material **1**, **2,** and **3**, respectively, was placed between two ITO conductive glass slides, heated at 51 °C, and compressed to prepare a uniform film with a rectangular surface area of 0.25 cm^2 and approx. 50 µm thickness. The conductivity experiments were performed in a two-electrode system by applying a constant potential (− 2 V) between the two ITO electrodes. The flowing current in the external electrical circuit was monitored upon the time while the temperature was ramped with 4 °C min^{-1} in the range from 30 to 90 °C.

Results and discussion

Synthesis

The ionic complexes **1**, **2,** and **3** were synthesized by salt metathesis reaction between the analogs viologen derivatives **1–3** as iodine salts and cesium 3,4,5-tris(dodecyloxy)benzene sulfonate (CsDOBS), respectively. The corresponding reagents were synthesized according to a literature procedure [21, 22].

During the ionic exchange reaction, the color of the organic phase changed from colorless to yellow, which is attributed to the transfer of viologen

dication from the aqueous to chloroform phase. The ionic complexes, formed between dicationic viologens **1–3** and 3,4,5-tris(dodecyloxy)benzene sulfonate, were isolated from the organic phase in excellent yield (> 93%) and characterized using ^{1}H-, ^{13}C-NMR and IR spectroscopy. (cf. SI for detailed spectroscopic data). Their purity exceeded 98% accordingly with elemental analysis results. Viologen^{2+}/DOBS^{-} ratio was deduced from the relative integral peaks of the respective ionic components and was found to be 1/2 (Fig. 1). The experimentally determined value of Viologen^{2+}/DOBS^{-} ratio in the corresponding ionic complex demonstrates that: (i) the interaction between Viologen^{2+} and DOBS^{-}, respectively, is electrostatic as per one unit of Viologen^{2+} it is required theoretically two DOBS^{-} units to ensure electrostatic neutrality, and (ii) the phase transfer reaction occurred quantitatively until the dicationic viologen from chloroform solution completely replaced the cesium.

Thermotropic behavior

Thermal properties of ionic complexes **1–3** were investigated using differential scanning calorimetry (DSC) and thermo-optical polarizing microscopy (TOPM). A comparison with the previously reported analog **MV** [12] was performed in order to understand the influence of nucleobases capping groups on the thermal behavior of ionic complexes **1–3**.

Figure 2a–c illustrates the corresponding 2nd heating–cooling cycles of ionic complexes **1–3**. At 8.2 °C for 1, − 17.7 °C for 2, and − 24 °C for 3, respectively, the endothermic peak corresponds to the melting transition from crystalline to mesophase state. Figure 2d–f shows the optical micrographs of derivatives **1–3** at 110 °C. The colored domains seen between the cross-polarizers above melting transition indicate that all three nucleobase-appended viologens exhibited optical anisotropy. Shearing experiments performed by mutual sliding of the microscope slides proved the liquid nature of the observed material; hence, the compounds are in a mesomorphic state.

The transition from crystal to LC state of all three complexes that occurred at low temperature was compared to analog, derivative **MV^{2+}(DOBS)2** (T_{m} = 64.7 °C) [12]. This is attributed to the presence of thymine and adenine in the mesogenic unit's chemical structure, which influence the supramolecular arrangement, i.e., destabilize the crystalline state.

The undisturbed texture of the mesophase, as obtained by cooling from the isotropic state, has been obtained only for compound **1** (Fig. 2d), which is the only ionic complex stable up to its isotropization temperature. The fan-like texture of **1** suggests a columnar type mesophase, an expectable supramolecular arrangement for a discotic mesogen such as 3,4,5-tris(dodecyloxy)benzene sulfonate anion [22]. Notably, the mesophase texture is different from the analog **MV** [16] revealing the influence of thymine capping units on supramolecular arrangement. The isotropization of **1** (192 °C) occurred at a lower temperature than **MV** (T_{iso} = 270 °C).

The compounds containing adenine as capping groups (**2** and **3**) were not thermally stable up to the isotropization point. They changed the color irreversibly into dark brown at elevated temperatures (> 160 °C) concomitantly with the loss of optical anisotropy. For this reason, it was impossible to

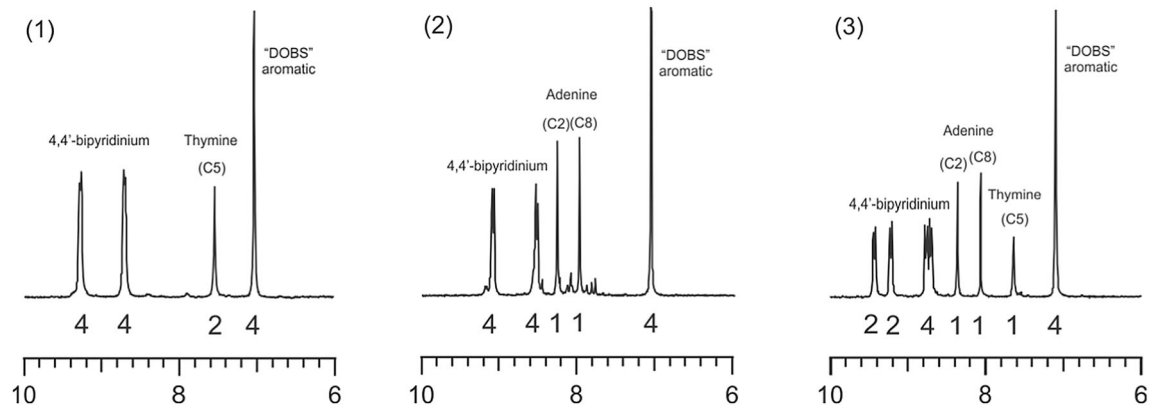

Figure 1 ^{1}H-NMR spectra in the aromatic region of the ionic complexes **1–3** in THF-d_8:D_2O (4:1 vol).

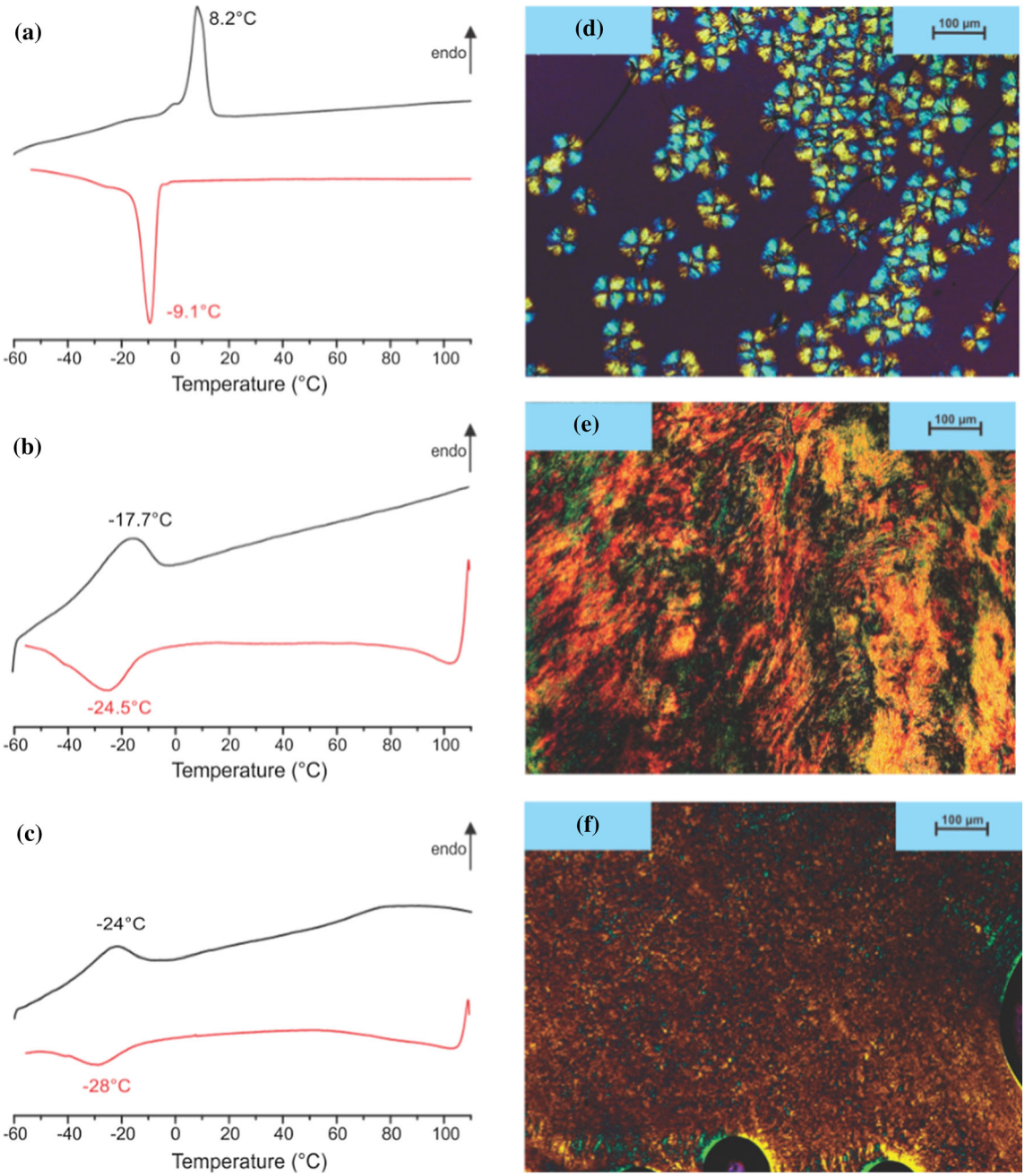

Figure 2 Second heating–cooling cycle of **1** (**a**), **2** (**b**), and **3** (**c**), respectively, at dT/dt = 10 K/min and the corresponding optical micrographs (**d**, **e** and **f**, respectively) at 110 °C between cross-polarizers.

obtain an undisturbed texture with characteristic features of the mesophase by cooling from the isotropic state. Ionic complexes 2 and 3 are thermally unstable due to irreversible oxidation of adenine in a media containing a suitable electron acceptor such as viologen. Irreversible electro/oxidation of adenine is well known and follows a complex mechanism [23, 24]. TGA analysis showed the ionic complexes losing mass at 296 °C for compound **1**, 306 °C for **2,** and 300 °C for compound **3** (cf. supporting information).

The phase transition schemes of derivatives **1–3** are summarized in Table 1.

Table 1 Phase transition temperatures and corresponding enthalpies of ionic complexes 1–3

Compound	Phase transition scheme[a]
(1)	Cr, 8.2 (35) Φ, 192 I[b]
(2)	Cr, -17.7 (22.5) Φ[c]
(3)	Cr, -24 (27.5) Φ[c]

[a]Transition temperatures (°C) and enthalpies (kJ/mol, in parentheses) determined by DSC during the 2nd heating run; [b]Isotropization temperature determined by thermo-optical analysis; [c]Thermally unstable beyond 160 °C; Cr = solid crystal, Φ = mesophase, *I* = isotropic phase

Self-association by hydrogen bonding in low-polar solvents

Ionic complexes of 4,4′-bipyridinium capped by nucleobases with amphiphilic anion $DOBS^-$ are expected to self-associate in solvents with low polarity due to the ability of nucleobase moieties to undergo in-plane hydrogen bonding. The self-association of ionic complexes **1–3** were investigated in solution by ^{1}H-NMR spectroscopy (i.e., one-dimensional ^{1}H-NMR and DOSY) and compared with nucleobase-free **MV**. The influence of solvent nature, temperature, and concentration were systematically checked.

The ^{1}H-NMR spectra at 30 °C in deuterated chloroform of the individually ionic complexes **1–3** and **MV**, respectively, are represented in Fig. 3. Except for the compound **MV**, all the other ionic complexes showed a line broadening of the spectra, increasing in order **1** < **3** < **2**.

The ^{1}H-NMR line broadening effect arises from the self-association of the molecules into higher molecular weight aggregates [25]. Previous research showed that thymine (T) and adenine (A) nucleobases could undergo many hydrogen bonding motifs in low-polar solvents. These motifs include self-associated cyclic dimers T–T, A–A, trimer A–A–A (k_{ass} < 4 M^{-1}), or complementary T–A base-pairing with higher association constant (k_{ass} > 100 M^{-1}) [26–30]. Our results show that the self-association of nucleobase-appended viologens in solvents with low polarity is induced by adenine and thymine, which are capable of hydrogen bonding.

The magnitude of signal attenuation seen in ^{1}H-NMR spectra is interpreted as a qualitative appreciation of the self-association degree. Comparing the relative signal broadening of the ionic complexes **1–3** (Fig. 3), the compound with the highest degree of self-association is **2**, containing two adenine units, while the ionic complex with the lowest degree of self-association is **1** containing two thymine units. The ionic complex **3**, comprising an adenine and a thymine group, has an intermediary self-association degree. Remarkably, the ionic complexes capped by adenine units exhibited the highest degree of self-association. This is explained by the nature of purinic adenine moiety, which contains more hydrogen bonding sites over the thymine [28], which enhances the supramolecular self-assembly process of the corresponding nucleobase-appended viologens.

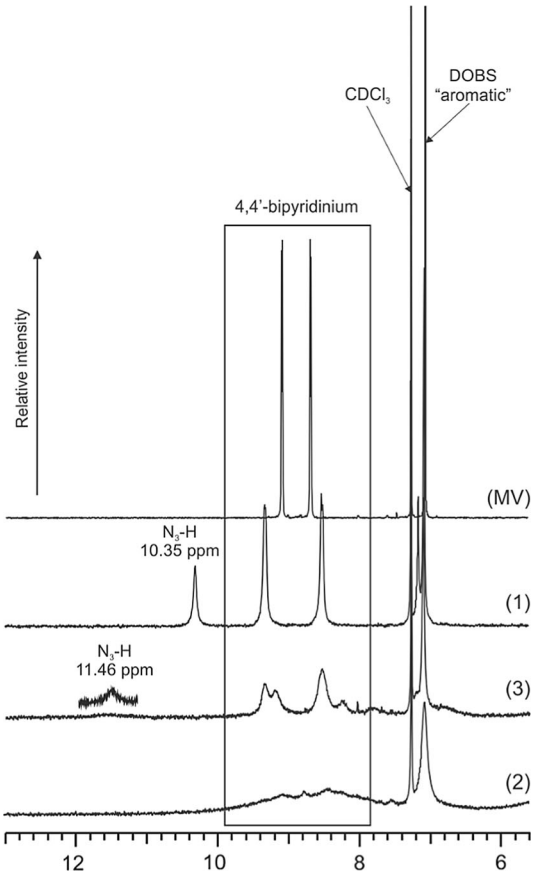

Figure 3 ^{1}H-NMR spectra in the aromatic region of the ionic complexes **1–3** (50 mM) in $CDCl_3$ at 30 °C.

Imino proton of thymine in compound **3** (N_3–H, 11.46 ppm, ma inset in Fig. 3) appeared broadened, and downfield shifted compared to *imino* proton (N_3–H, 10.35 ppm) in compound **1**. This observation suggests that the thymine unit in compound **3** is associated with hydrogen bonding with the complementary adenine.

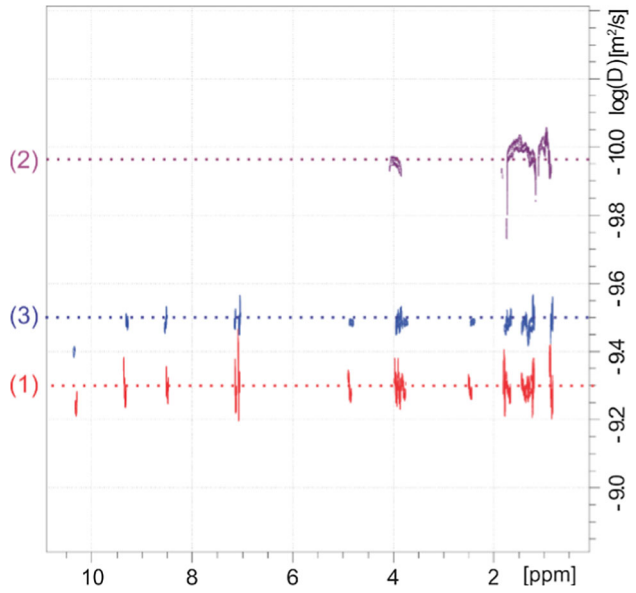

Figure 4 Overlapped DOSY spectra of ionic complexes **1**–**3** (50 mM) in $CDCl_3$ at 30 °C.

An overlap of the three individual DOSY spectra of ionic complexes **1**, **2,** and **3**, respectively, in $CDCl_3$ at 30 °C, is shown in Fig. 4. The diffusion coefficients of the ionic complexes increase in the order **1** < **3** < **2**. The observed difference in the diffusion of ionic complexes **1–3** is explained by the different self-association degrees. This trend is in complete agreement with the assumption derived from previously presented one-dimensional ^{1}H-NMR experiments.

The self-association by hydrogen bonding of ionic complexes **1–3** is an equilibrium process. The molar ratio of associated and non-associated molecular species depends on the thermodynamic parameters (temperature, concentration) and association constant (K_{ass}). In respect to this, a series of DOSY experiments were performed to investigate the influence of thermodynamic parameters, i.e., temperature and concentration. Figure 5 shows the measured diffusion coefficients of compound **2** as a function of temperature and concentration. From the trend of diffusion coefficients, it can be concluded: (1) by temperature increase, the self-association degree decreases because of thermal-induced hydrogen bond breaking, and (2) by concentration increase, the self-association degree of the molecular species increases.

Further on, it was investigated the self-association behavior of ionic complexes **1–3** in three different solvent media: chloroform, THF, and a mixture of THF: water (4:1 volume ratio) (see Fig. 6). The highest

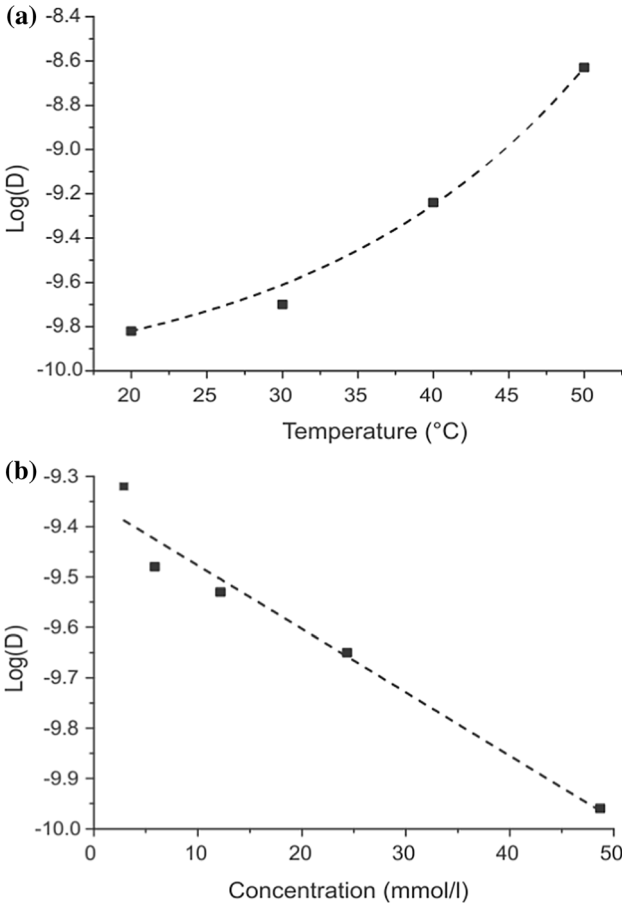

Figure 5 Plot of diffusion coefficient (logD) as a function of **a** temperature and **b** concentration for deriv. **2** in THF-d_8.

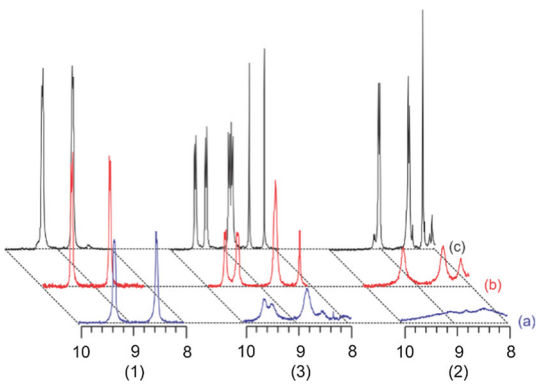

Figure 6 ^{1}H-NMR spectra in the aromatic region of the ionic complexes **1**–**3** at 30 °C in **a** $CDCl_3$, **b** THF-d_8, and **c** THF-d_8:D_2O (4:1 vol).

degree of self-association was observed in chloroform, where peak signals of respective ionic complexes appeared significantly diminished and broadened compared with the other two solvent systems. In THF, a solvent with higher polarity than

chloroform, the ionic complexes exhibited a lower broadening of the peaks suggesting a lower degree of self-association. When the solvent was a mixture of THF: water, practically no self-association occurred since no line broadening was observed. The self-association of nucleobase-appended viologens was inhibited in THF: water, obviously due to the competitive hydrogen bonding with water molecules [31–33].

Combined experiments, DOSY, and one-dimensional ^{1}H-NMR proved that the self-association of nucleobase-appended viologens **1–3** is a process strongly influenced by the type of nucleobase (thymine or adenine), solvent media as well as by the thermodynamic parameters, temperature, and concentration. The crucial role of nucleobases in the self-association behavior of complexes **1–3** was highlighted by direct comparison with the analogs derivative **MV,** which did not self-associate in the same environmental conditions. It is noteworthy that viologens capped dihexadecylviologen bistriflimide can self-associate by electrostatic forces in low-polar solvents [34]. In our system, the self-association by electrostatics was insignificant, presumably due to a much bulky counter anion DOBS.

Electrochemical properties

Electrochemical characterization of solution of **1–3** was performed to regard the influence of the self-association process on the redox properties of the 4,4′-bipyridinium unit. The compounds **1–3** and analog, derivative **MV**, respectively, were investigated by means of cyclic voltammetry.

The cyclic voltammograms in Fig. 7 represent the typical reversible reduction process of the 4,4′-bipyridinium unit from dicationic state (V^{2+}) to radical cation ($V^{+\bullet}$) and further to the neutral species (V^{0}). The cathodic and anodic current peaks (Ipc/Ipa) ratio was determined after baseline correction of the corresponding cyclic voltammograms and satisfies the condition for reversibility ($I_{pc}/I_{pa} = 1$) for all ionic complexes. Separation peak potential ($\Delta E = E_{pa} - E_{pc}$) for both reduction steps overcome the value required for the one-electron transfer process (< 59 mV). We believe this effect is attributed to the iR drop rather than to the reversibility of the electrochemical process. The iR drop is expected in a solvent with low dielectric permittivity, such as THF [35].

Derivatives **1–3** were reduced at much positive potential than the analogs derivatives **MV**. The value of formal potentials $E^{0}1$ and $E^{0}2$, respectively, of ionic complexes **1–3** followed the same trend as for the analogs derivatives as PF_6^- salt [21] and were not affected by the self-assembly process in THF.

The linear trend of the plot of current peak I_{pc1} against the square root of the scan rate indicates a diffusion-controlled redox process in the range from 0.05 to 1 V·s^{-1}. The limiting process is related *to* the electron transfer kinetics between the electrode and the redox species. Remarkably, the rate of electron transfer was diminished as a result of the self-

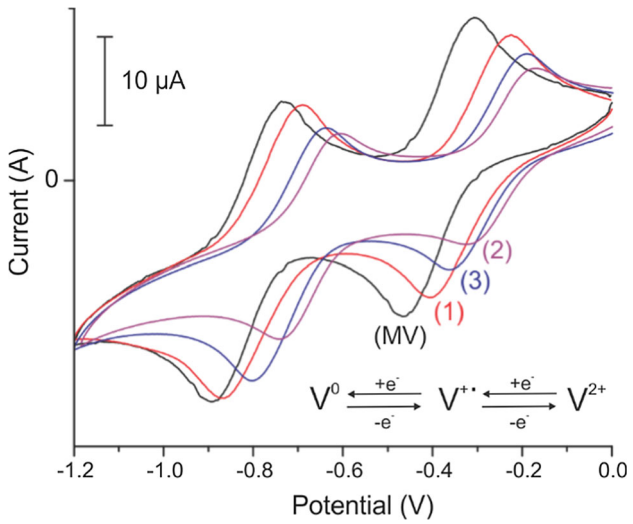

Figure 7 Cyclic voltammograms of (0.001 mol L^{-1}) ionic complexes **1**–**3** and **MV**, respectively, at 0.6 V·s^{-1} scan rate in LiTFSI/THF (0.1 mol L^{-1}).

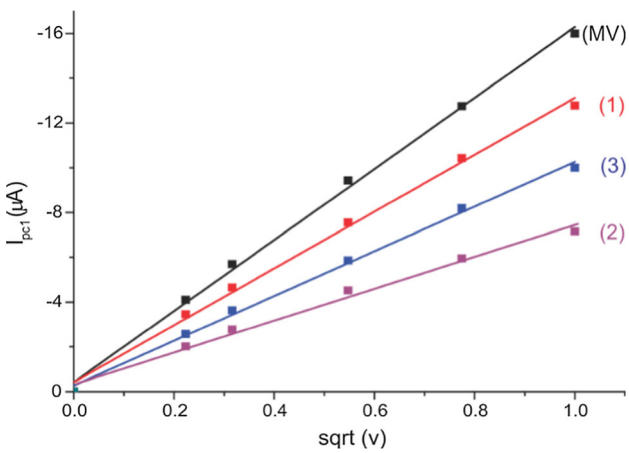

Figure 8 Plot of the first peak current (I_{pc1}) versus the square root of the scan rate (v) for **1**–**3** and **MV**, respectively.

association process. That is reflected in the small value of the slope for derivatives **1–3** compared to analog **MV** (Fig. 8).

The diffusion coefficients calculated from cyclic voltammetry data (D_{CV}) of ionic complexes **1–3** and **MV**, respectively, increase in the order **2** < **3** < **1** < **MV** and follow the same trend as DOSY experiments. Detailed electrochemical parameters derived from CV measurements can be found in supporting information.

Ionic conductivity and thermochromism in solid state

Figure 9a illustrates two different temperature ranges with distinctive ionic conductive properties. In the first low temperature range below 60 °C, no passing current between the electrodes was observed. The ionic complexes **1–3** are highly viscous. The ionic mobility is moderate; they act as insulator materials; In the second temperature range above 60 °C, complexes **1–3** are less viscous, and the conductivity increases exponentially with the temperature. In this temperature regime, the ionic complexes **1–3** behaved as 2nd order conductors. The 2nd order conductors are defined as materials of which electrical conductivity increases with the increase in temperature.

Figure 9b presents the Arrhenius plot of conductivity in the high-temperature regime (above 60 °C) for the ionic complexes **1–3**, respectively. The activation energy (E_a) was calculated with Formula 1 [36]:

$$E_a = -(m \cdot R) \quad (1)$$

where m is the slope of the Arrhenius plot (1000 K), and R is the gas constant (8.314 J K^{-1} mol^{-1}). The activation energy values were 65.85 kJ/mol for **1**, 71.67 kJ mol^{-1} for **2,** and 74.41 kJ mol^{-1} for **3**. When a compact film of compounds **1**, **2**, and **3**, respectively, was heated between two glass plates without any applied voltage, a color change was observed. The corresponding materials 1–3 changed the color instantly (small ΔT) from pale-yellow to blue-green above 110 °C (Fig. 10). Similar behavior was previously reported for the analog, derivative **MV** [16].

Figure 11 illustrates the Vis spectra of the thin films of respective compounds **1–3** after exposure at 110 °C between two glass plates without any applied voltage. The typical absorption band with a maximum wavelength of 600 nm demonstrates the formation of monomeric radical and cationic species ($V^{+\bullet}$). The oxidation of the film in the presence of atmospheric oxygen (color change from blue-green to yellow) occurred when the film was cooled down at room temperature (approx. 21 °C) and stand for more than 12 h. It is noteworthy that the color change did not occur at the outer rim of the thin films where contact with the air is imminent, and the formed radical species are spontaneously oxidized back in the presence of the atmospheric oxygen.

Above 60 °C, the liquid crystalline compounds **1–3** started to behave as 2nd order conductors because of the exponential increase in ionic mobility. Under these conditions, the electron transfer from the anion

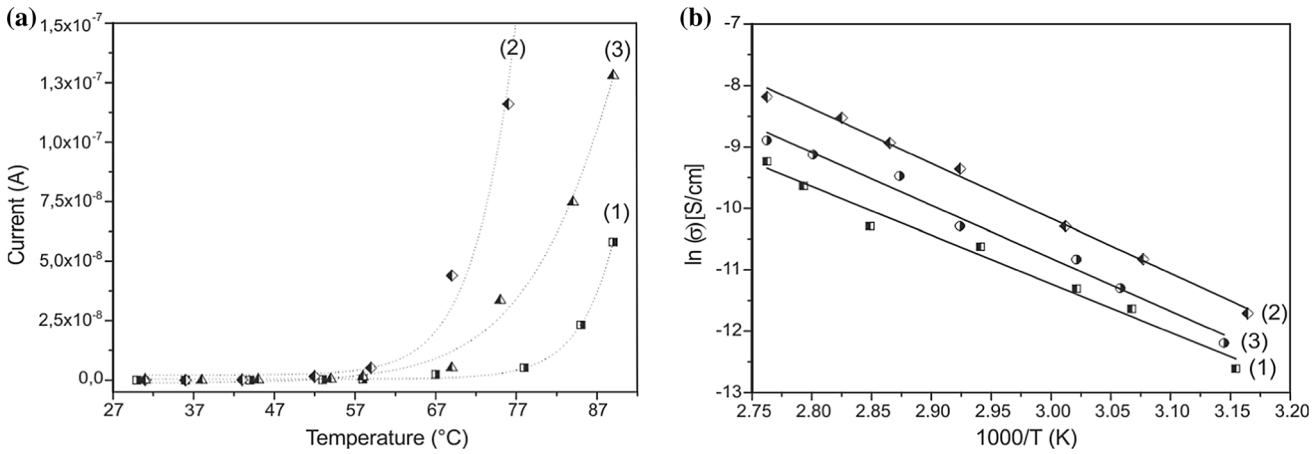

Figure 9 **a** Plot of current versus temperature at a constant applied voltage (− 2 V) for ionic complexes **1**–**3**; **b** Arrhenius plots of ionic conductivity versus reciprocal temperature for ionic complexes **1**–**3**.

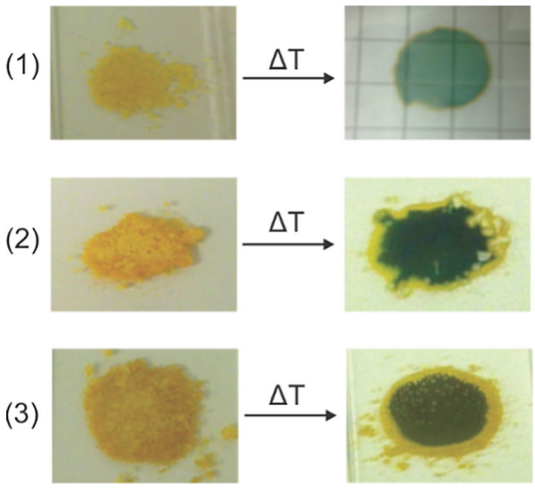

Figure 10 Ionic complexes **1**–**3** compressed between two glass slides, before and after thermal treatment.

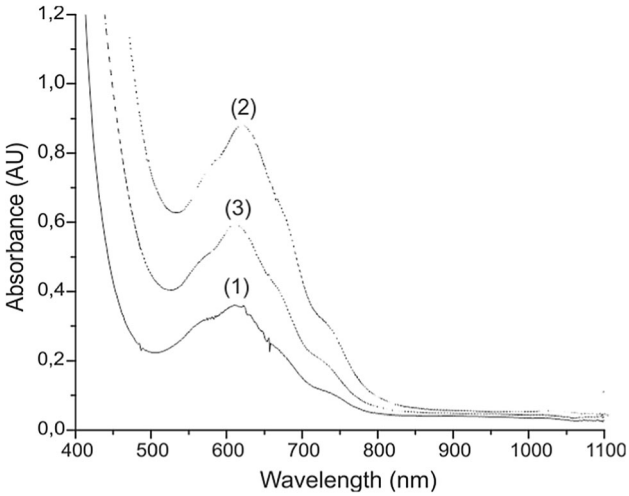

Figure 11 VIS spectra of a thin film of ionic complexes **1**–**3** after exposure to 110 °C.

3,4,5-tris(dodecyloxy)benzene sulfonate, which acts as an electron donor source, to the viologen moiety (electron acceptor) is facilitated. Extensive work of Haramoto et al. [37] and Nanasawa et al. [3] also demonstrated that the long alkylbenzene sulfonate counter anion might act as an electron source for photoreduction N,N′-diphenyl bipyridinium derivatives in LC state. On the other hand, the group of Kato [38, 39] concluded that the mobility of the ionic species plays a crucial role in the redox activity of the liquid crystal materials combining ionic and electronic functions. Beneduci et al. [40] emphasized the importance of ionic conductivity on the electrochromic properties in the bulk state of the π-conjugated thienoviologens liquid crystals, compounds with similar redox activity such as the one reported in our study. Remarkably, the electrochromic reaction of derivatives **1**–**3** did not require any external applied potential like the nanostructured redox liquid crystals reported by Kato or Beneduci [27–29]. The reduction of viologen units occurred spontaneously at a temperature at which the material existed in LC state with sufficiently low viscosity to allow the charge transport in the bulk liquid crystal.

Conclusions

A novel class of redox-active liquid crystalline materials (**1**–**3**) capable of self-associating in solution by hydrogen bonding was synthesized and characterized concerning structure, self-assembly, and physicochemical properties. Such materials are based on ion pairing of amphiphilic anion 3,4,5-tris(dodecyloxy)benzene sulfonate (**DOBS**$^-$) with dicationic nucleobase-appended viologens. The compounds **1**–**3** exhibited liquid crystalline properties at room temperature, while the analogs *paraquat* derivative **MV** changed from solid crystalline to LC state above 60 °C. The fan-shaped texture of compound **1**, observed on a polarized light microscope, suggested a columnar type mesophase different from that reported for **MV** analog [12]. Compound **1**, containing thymine units in its structure exclusively, exhibited a stable mesophase until isotropization. By contrast, compounds **2** and **3** were decomposed by the temperature before transition into the isotropic state, revealing the influence of adenine on the thermal instability. Derivatives **1**–**3** self-associate in solvents with low polarity by hydrogen bonding. ^{1}H-NMR and DOSY experiments demonstrated that the degree of self-association depends strongly on the nature of the capping groups (i.e., thymine or adenine), solvent polarity, temperature, and concentration. Due to self-association by hydrogen bonding in solution, the electron transfer rate during electrochemical reduction of **1**–**3** was significantly diminished. The ionic complexes **1**–**3** behaved as 2nd order conductors in the mesophase state, at a temperature at which viscosity increased significantly as well as theirs analog **MV** derivative. Ionic mobility, induced by thermal energy, facilitated the electron transfer from the anion **DOBS**$^-$ to the viologen unit, which was readily transformed in the radical, cationic state

under anaerobic conditions. Compounds 1–3 show thermochromic and ionic conductive properties similarly to MV but in mild temperature conditions. The new class of compounds, combining the hydrogen bonding abilities of nucleobases, redox function of viologen, and thermotropic properties of dodecyl sulfonate, has a great potential for the construction of optoelectronic components for optoelectronic devices.

Funding

Open Access funding enabled and organized by Projekt DEAL. The authors did not receive support from any organization for the submitted work. No funds, grants, or other support were received for conducting this study.

Declarations

Conflict of interests The authors declare that they have no known competing financial interests or personal relationships that could have influenced the work reported in this paper. All authors certify that they have no affiliations with or involvement in any organization or entity with any financial or non-financial interest in the subject matter or materials discussed in this manuscript. The authors have no financial or proprietary interests in any material discussed in this article.

Supplementary Information: The online version contains supplementary material available at https://doi.org/10.1007/s10853-021-06554-1.

References

[1] Choi SY, Mamak M, Coombs N et al (2004) Electrochromic performance of viologen-modified periodic mesoporous nanocrystalline anatase electrodes. Nano Lett 4:1231–1235. https://doi.org/10.1021/nl049484d

[2] Campus F, Bonhote P, Grätzel M et al (1999) Electrochromic devices based on surface-modified nanocrystalline TiO_2 thin-film electrodes. Sol Energy Mater Sol Cells 56:281–297

[3] Nanasawa M, Matsukawa Y, Jin JJ, Haramoto Y (1997) Redox photochromism of viologen in organized solid state. J Photochem Photobiol A 109:35–38. https://doi.org/10.1016/S1010-6030(97)00105-6

[4] Sun J-K, Wang P, Yao Q-X et al (2012) Solvent- and anion-controlled photochromism of viologen-based metal–organic hybrid materials. J Mater Chem 22:12212–12219. https://doi.org/10.1039/c2jm30558e

[5] Kinuta T, Sato T, Tajima N et al (2010) Solid-state thermochromism observed in charge-transfer complex composed of binaphthol and viologen. J Mol Struct 982:45–49. https://doi.org/10.1016/j.molstruc.2010.07.048

[6] Li X-N, Tu Z-M, Li L et al (2020) A novel viologen-based coordination polymer with multi-stimuli responsive chromic properties: photochromism, thermochromism, chemochromism and electrochromism. Dalton Trans 49:3228–3233. https://doi.org/10.1039/C9DT04699B

[7] Sui Q, Ren X-T, Dai Y-X et al (2017) Piezochromism and hydrochromism through electron transfer: new stories for viologen materials. Chem Sci 8:2758–2768. https://doi.org/10.1039/C6SC04579K

[8] Papadakis R (2019) Mono- and di-quaternized 4,4′-bipyridine derivatives as key building blocks for medium- and environment-responsive compounds and materials. Molecules 25:1. https://doi.org/10.3390/molecules25010001

[9] Hoogvliet JC, Lievense LC, Dijk C, Veeger C (1988) Electron transfer between the hydrogenase from Desulfovibrio vulgaris (Hildenborough) and viologens. 1. Investigations by cyclic voltammetry. Eur J Biochem 174:273–280. https://doi.org/10.1111/j.1432-1033.1988.tb14094.x

[10] Krishnamurthy S, Lightcap IV, Kamat PV (2011) Electron transfer between methyl viologen radicals and graphene oxide: reduction, electron storage and discharge. J Photochem Photobiol A 221:214–219. https://doi.org/10.1016/j.jphotochem.2011.02.024

[11] Moore JS, Stupp SI (1986) Charge-transfer and thermochromic phenomena in solid polyelectrolytes. Macromolecules 19:1815–1824. https://doi.org/10.1021/ma00161a007

[12] Monk PMS, Hodgkinson NM, Partridge RD (1999) The colours of charge-transfer complexes of methyl viologen: effects of donor, ionic strength and solvent. Dyes Pigm 43:241–251. https://doi.org/10.1016/S0143-7208(99)00063-7

[13] Binnemans K (2005) Ionic liquid crystals. Chem Rev 105:4148–4204. https://doi.org/10.1021/cr0400919

[14] Axenov KV, Laschat S (2011) Thermotropic ionic liquid crystals. Materials 4:206–259. https://doi.org/10.3390/ma4010206

[15] Zheng Y, Wang J, Tang X et al (2020) Liquid-crystalline behavior and ferroelectric property of viologen-based ionic liquid crystals. J Mol Liq 301:112369. https://doi.org/10.1016/j.molliq.2019.112369

[16] Asaftei S, Ciobanu M, Lepadatu AM et al (2012) Thermotropic ionic liquid crystals by molecular assembly and ion pairing of 4,4′-bipyridinium derivatives and tris(dodecyloxy)benzenesulfonates in a non-polar solvent. J Mater Chem 22:14426–14437. https://doi.org/10.1039/c2jm31830j

[17] Tanabe K, Yasuda T, Yoshio M, Kato T (2007) Viologen-based redox-active ionic liquid crystals forming columnar phases. Org Lett 9:4271–4274. https://doi.org/10.1021/ol701741e

[18] Casella G, Causin V, Rastrelli F, Saielli G (2014) Viologen-based ionic liquid crystals: induction of a smectic A phase by dimerisation. Phys Chem Chem Phys 16:5048–5051. https://doi.org/10.1039/C3CP54628D

[19] Casella G, Causin V, Rastrelli F, Saielli G (2016) Ionic liquid crystals based on viologen dimers: tuning the mesomorphism by varying the conformational freedom of the ionic layer. Liq Cryst 43:1161–1173. https://doi.org/10.1080/02678292.2016.1161852

[20] Bhowmik PK, Al-Karawi MKM, Killarney ST et al (2020) Thermotropic liquid-crystalline and light-emitting properties of bis(4-aalkoxyphenyl) viologen bis(triflimide) salts. Molecules 25:2435. https://doi.org/10.3390/molecules25102435

[21] Ciobanu M, Asaftei S (2015) Nucleobase appended viologens: building blocks for new optoelectronic materials. Opt Mater 42:262–269. https://doi.org/10.1016/j.optmat.2014.12.044

[22] Beginn U, Yan L, Chvalun SN et al (2008) Thermotropic columnar mesophases of wedge-shaped benzenesulfonic acid mesogens. Liq Cryst 35:1073–1093. https://doi.org/10.1080/02678290802376107

[23] Gonçalves LM, Batchelor-McAuley C, Barros AA, Compton RG (2010) Electrochemical oxidation of adenine: a mixed adsorption and diffusion response on an edge-plane pyrolytic graphite electrode. J Phys Chem C 114:14213–14219. https://doi.org/10.1021/jp1046672

[24] Abbaspour A, Noori A (2008) Electrochemical studies on the oxidation of guanine and adenine at cyclodextrin modified electrodes. Analyst 133:1664–1672. https://doi.org/10.1039/b806920

[25] Escuder B, LLusar M, Miravet JF (2006) Insight on the NMR study of supramolecular gels and its application to monitor molecular recognition on self-assembled fibers. J Org Chem 71:7747–7752. https://doi.org/10.1021/jo0612731

[26] Sivakova S, Rowan SJ (2005) Nucleobases as supramolecular motifs. Chem Soc Rev 34:9–21. https://doi.org/10.1039/b304608g

[27] Bazzi HS, Sleiman HF (2002) Adenine-containing block copolymers via ring-opening metathesis polymerization: synthesis and self-assembly into rod morphologies. Macromolecules 35:9617–9620. https://doi.org/10.1021/ma025676o

[28] Biemann L, Häber T, Maydt D et al (2008) Structural assignment of adenine aggregates in CDCl3. J Chem Phys 128:195103. https://doi.org/10.1063/1.2912064

[29] Wilson AJ (2007) Non-covalent polymer assembly using arrays of hydrogen-bonds. Soft Matter 3:409–425. https://doi.org/10.1039/b612566b

[30] Kyogoku Y, Lord RC, Rich A (1967) The effect of substituents on the hydrogen bonding of adenine and uracil derivatives. Proc Natl Acad Sci 57:250–257. https://doi.org/10.1073/pnas.57.2.250

[31] Spencer JN, Campanella CL, Harris EM, Wolbach WS (1985) Solvent effects on hydrogen-bond formation. J Phys Chem 89:1888–1891. https://doi.org/10.1021/j100256a015

[32] Cook JL, Hunter CA, Low CMR et al (2007) Solvent effects on hydrogen bonding. Angew Chem Int Ed 46:3706–3709. https://doi.org/10.1002/anie.200604966

[33] Ouhib F, Raynal M, Jouvelet B et al (2011) Hydrogen bonded supramolecular polymers in moderately polar solvents. Chem Commun 47:10683–10685. https://doi.org/10.1039/c1cc14590h

[34] Li S, Saielli G, Wang Y (2018) Aggregation behavior of dihexadecylviologen bistriflimide ionic liquid crystal in different solvents: influence of polarity and concentration. Phys Chem Chem Phys 20:22730–22738. https://doi.org/10.1039/C8CP03055C

[35] Funston A, Kirby JP, Miller JR et al (2005) One-electron reduction of an “extended viologen” *p* -phenylene-bis-4,4 ’-

(1-aryl-2,6-diphenylpyridinium) dication. J Phys Chem A 109:10862–10869. https://doi.org/10.1021/jp053556n

[36] Bockris JO, Reddy AKN, Bockris JO (1998) Ionics, 2nd edn. Plenum Press, New York

[37] Haramoto Y, Yin M, Matukawa Y et al (1995) A new ionic liquid crystal compound with viologen group in the principal structure. Liq Cryst 19:319–320. https://doi.org/10.1080/02678299508031986

[38] Yazaki S, Funahashi M, Kato T (2008) An electrochromic nanostructured liquid crystal consisting of π-conjugated and ionic moieties. J Am Chem Soc 130:13206–13207. https://doi.org/10.1021/ja805339q

[39] Yazaki S, Funahashi M, Kagimoto J et al (2010) Nanostructured liquid crystals combining ionic and electronic functions. J Am Chem Soc 132:7702–7708. https://doi.org/10.1021/ja101366x

[40] Beneduci A, Cospito S, La Deda M et al (2014) Electrofluorochromism in π-conjugated ionic liquid crystals. Nat Commun 5:3105. https://doi.org/10.1038/ncomms4105